



ELSEVIER

Journal of Non-Crystalline Solids 168 (1994) 223–231

JOURNAL OF  
NON-CRYSTALLINE SOLIDS

# Optical absorption of copper phosphate glasses in the visible spectrum

Byeong-Soo Bae, Michael C. Weinberg \*

*Department of Materials Science and Engineering, University of Arizona, Tucson, AZ 85721, USA*

(Received 10 June 1993; revised manuscript received 26 August 1993)

## Abstract

Optical absorption of copper phosphate glasses with batch compositions of 40, 50 and 55 mol% CuO have been examined in the visible and near-infrared range as a function of  $[\text{Cu}^{2+}]/[\text{Cu}_{\text{total}}]$  in the glasses. An absorption band centered at about  $11\,000\text{ cm}^{-1}$  is produced due to an octahedral coordination of  $\text{Cu}^{2+}$  in the glass with strong tetragonal distortion. This absorption band is resolved into three-component Gaussian bands around 8500, 12000 and  $13\,250\text{ cm}^{-1}$ . These bands are assigned to the energy transitions  ${}^2\text{A}_{1g} \rightarrow {}^2\text{B}_{1g}$ ,  ${}^2\text{B}_{2g} \rightarrow {}^2\text{B}_{1g}$  and  ${}^2\text{E}_g \rightarrow {}^2\text{B}_{1g}$ , respectively. The degree of tetragonal distortion of  $\text{Cu}^{2+}$  coordination is slightly enhanced with increases in the  $[\text{Cu}^{2+}]$  ratio and CuO content. A minimum absorption in the visible spectrum is produced by overlapping of the absorption bands of  $\text{Cu}^{2+}$  and  $\text{Cu}^{1+}$ . The position of the minimum absorption shifts to higher wavenumber with increasing  $[\text{Cu}^{2+}]$  ratio in the glass regardless of glass composition and is responsible for color changes.

## 1. Introduction

Since the incorporation of transition metal ions into glass creates color in the glass, transition metal ions have been used as color centers in glass. Thus, the optical absorption of glasses containing transition metal ions (including copper ions) has been studied to explore their coloring mechanisms in different glass systems [1–20]. The electronic structure of the copper atom is  $3d^{10}4s^1$ , and the usual oxidation states are  $\text{Cu}^0$ ,  $\text{Cu}^{1+}$  and  $\text{Cu}^{2+}$ . The  $\text{Cu}^{2+}$  ion has partially filled d orbitals creating color centers in glass via an absorption band in the visible spectrum. Thus, most glasses

which contain  $\text{Cu}^{2+}$  have a blue to green color. Colors produced in glasses by  $\text{Cu}^{2+}$  have been interpreted from the point of view of ligand field theory [1–3]. The octahedral coordination of  $\text{Cu}^{2+}$  in glass produces a ligand field splitting of the free ion energy level. The absorption band in the visible spectrum associated with the copper containing glasses is a result of energy transitions between these perturbed energy levels.

Studies of the variations in optical absorption band in the visible and near-infrared region of the spectrum with glass composition have been made previously [3–20]. However, most investigations of optical absorptions have been restricted to the glasses doped with copper as a color center, since the absorption coefficient of  $\text{Cu}^{2+}$  is very high in glasses. The absorption band is quite sensitive to the glass-forming ions present in the

\* Corresponding author. Tel: +1-602 621 6909. Telefax: +1-602 621 8059.

glass, and its peak position is located around 850 nm in phosphate glasses [15–20]. Also, the peak position, shape and extinction coefficient of the absorption vary with the glass modifier content. In addition, the asymmetry and width of the absorption band has been demonstrated to be due to the presence of two or more overlapping absorption bands produced by the tetragonal distortion of the octahedral coordination of  $\text{Cu}^{2+}$  in glass [3,4,6,14]. This visible absorption band has been deconvoluted into two-component absorption bands in silicate, borate and nitrate glasses. The positions of the deconvoluted absorption bands have been found to be dependent upon the composition.

The optical absorption of copper phosphate glasses in the visible region of the spectrum is investigated in this work. These glasses have a large copper content and consequently are deeply colored glasses exhibiting extremely high optical absorption in the visible–near-infrared region of the spectrum. As mentioned, the  $\text{Cu}^{2+}$  in an octahedral field with a strong tetragonal distortion has been found to be responsible for this absorption.  $\text{Cu}^{1+}$  has also been shown to create optical absorption bands in phosphate glasses [21,22]. These optical absorption bands in copper phosphate glasses are centered in the UV region, but their tails extend into the visible. Thus, the minimum absorption in copper phosphate glasses is located between the absorption band and UV absorption edge. The position of this minimum absorption has been shown to shift toward higher

energy with increase in the  $[\text{Cu}^{2+}]/[\text{Cu}_{\text{total}}]$  ratio, which will be called the  $[\text{Cu}^{2+}]$  ratio [20].

The objectives of the present study are: (1) to explain the color of copper phosphate glasses, as functions of the  $[\text{Cu}^{2+}]$  ratio and glass composition, via investigation of their optical absorption spectra; (2) to elucidate the features of the absorption band of copper phosphate glasses and compare the latter with those obtained from the copper-doped glasses; (3) to obtain insights regarding changes in the  $\text{Cu}^{2+}$  environment as a function of the  $[\text{Cu}^{2+}]$  ratio in the glass and glass composition.

## 2. Experimental procedure

$\text{CuO-P}_2\text{O}_5$  glasses having compositions 40,50,55 mol%  $\text{CuO}$ , were prepared using analytical reagent grade  $\text{CuO}$  and  $\text{NH}_4\text{H}_2\text{PO}_4$  [23]. Glasses with different oxidation state ratios of copper were made by using various melting times. About 60 g of chemicals were mixed with isopropyl alcohol and dried to obtain homogenized batches. A quartz crucible (100 ml capacity) containing the batch was initially heated at  $500^\circ\text{C}$  for about 2 h in order to evaporate ammonia and water in the batch and minimize the tendency of subsequent phosphate loss. A quartz crucible was used since it was found that a quartz crucible was more inert than an alumina crucible [23]. The crucible was transferred to another furnace, which was preheated to the melting temperature of

Table 1  
Preparations and chemical analyses of glasses

Glass	Batch composition	Melting temperature ( $^\circ\text{C}$ )	Melting time	Annealing temperature ( $^\circ\text{C}$ )	$[\text{Cu}^{2+}]$ (wt%)	$[\text{Cu}^{2+}]/[\text{Cu}_{\text{total}}]$ (%)
A	50CuO · 50P <sub>2</sub> O <sub>5</sub>	1000	15 min	200	6.75 ± 1.70	22.3 ± 5.6
B		1000	30 min	200	15.20 ± 1.08	50.5 ± 3.6
C		1000	1 h	300	22.20 ± 0.84	74.0 ± 2.8
D		1000	2 h	400	27.35 ± 0.57	92.1 ± 1.9
E		1000	6 h	500	29.05 ± 0.29	99.5 ± 1.0
F	40CuO · 60P <sub>2</sub> O <sub>5</sub>	1000	30 min	200	12.49 ± 1.10	48.6 ± 4.3
G		1000	6 h	500	25.45 ± 0.21	99.8 ± 0.8
H	55CuO · 45P <sub>2</sub> O <sub>5</sub>	1100	30 min	200	18.92 ± 1.21	56.3 ± 3.6
I		1100	6 h	400	27.41 ± 0.93	82.3 ± 2.8

Table 2  
Characteristics of optical absorption spectra and colors of glasses

Glass	Absorption band peak wavenumber ( $\text{cm}^{-1}$ )	Extinction coefficient ( $1 \text{ mol}^{-1} \text{ cm}^{-1}$ ) at peak wavenumber	Minimum absorption wavenumber ( $\text{cm}^{-1}$ )	Color
A	10 800	74.95	16 129	tan
B	10 900	66.16	16 447	brown
C	11 000	58.35	17 182	yellow-green
D	11 100	61.21	17 731	green
E	11 100	69.78	18 248	blue
F	10 600	65.72	16 502	brown
G	11 000	57.24	18 182	blue
H	10 800	70.75	16 556	brown
I	11 500	63.00	17 241	green

1000°C. The batch was melted in air for 15 min to 6 h depending on the desired oxidation state ratio of copper in the glass. The melt was poured onto a clean copper plate and cast into a disc shape of about 3 cm diameter and of 3 mm thickness. The glasses were annealed for 5 h at 300°C–500°C depending on their  $[\text{Cu}^{2+}]$  ratio. All samples were stored in a vacuum desiccator to prevent moisture attack.

All samples were confirmed to be amorphous by X-ray diffraction and to be homogeneous by scanning electron microscopy and transmission electron microscopy. The concentrations of the total copper and  $\text{Cu}^{2+}$  were determined using complexometric titration previously described [24].

Due to the large absorption of the glasses, it was necessary to prepare thin samples for optical absorption spectroscopy measurements. The glass samples were ground and polished using SiC paper and 0.03  $\mu\text{m}$  alumina. The sample thicknesses were 40–60  $\mu\text{m}$ . The optical absorption measurements were made in the wavelength range 200–2500 nm using a Shimadzu UV-3100 UV-VIS-NIR spectrophotometer.

The compositions, melting and annealing conditions, and chemical analyses of the glasses which were prepared are given in Table 1. The actual compositions of the glasses may differ somewhat from the nominal composition due to vaporization of phosphorous, and this departure is larger for lower CuO content in glasses, as illustrated in previous work [23].

### 3. Results

Colors of the glasses with  $50\text{CuO} \cdot 50\text{P}_2\text{O}_5$  batch composition vary from tan to blue with increasing  $[\text{Cu}^{2+}]$  ratio in the glasses as shown in Table 2. Optical absorption spectra of the glasses are shown in Fig. 1. One observes a broad absorption band centered near  $11\,000 \text{ cm}^{-1}$  and a sharp increase in absorption (an absorption edge) at larger wavenumbers. The shape of the absorption band is similar regardless of the  $[\text{Cu}^{2+}]$  ratio of the glass, but the intensity and width of the absorption band is enhanced with increasing  $[\text{Cu}^{2+}]$  ratio. In addition, the absorption edge shifts to larger wavenumbers as the  $[\text{Cu}^{2+}]$  ratio in the glass grows. Thus, the minimum position of the absorption between the absorption band and

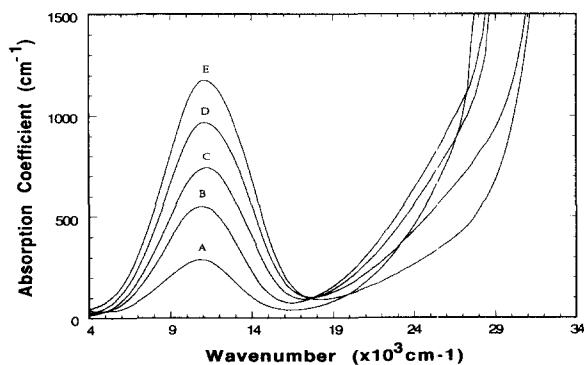


Fig. 1. Optical absorption spectra of glasses with 50% CuO batch composition having various  $[\text{Cu}^{2+}]$  ratios. A–E, see Table 1.

absorption edge (listed in Table 2) moves to larger wavenumbers for higher  $[\text{Cu}^{2+}]$  ratios in the glass.

For  $40\text{CuO} \cdot 60\text{P}_2\text{O}_5$  and  $55\text{CuO} \cdot 45\text{P}_2\text{O}_5$  batch composition glasses, the reduced glasses (F and H) are a brown color and the oxidized glasses (G and I) a green or blue color as shown in Table 2. Fig. 2 shows the optical absorption spectra of the glasses. All spectra exhibit absorption characteristics similar to those of  $50\text{CuO} \cdot 50\text{P}_2\text{O}_5$ . The absorption bands of the oxidized glasses are more intense and wider than those of the reduced glasses for each composition. The absorption edge changes depending on the glass composition and  $[\text{Cu}^{2+}]$  ratio in the glass. The absorption edge moves to larger wavenumbers with increasing  $[\text{Cu}^{2+}]$  ratio and decreasing CuO content in the glass. However, the wavenumber of the minimum absorption position listed in Table 2 increases with growing  $[\text{Cu}^{2+}]$  ratio in the glass, irrespective of the glass composition.

Extinction coefficients of absorption band peaks are calculated and listed in Table 2. The peak extinction coefficient is not constant with  $\text{Cu}^{2+}$  content in the glasses. Although these values contain some errors due to measurement errors in factors such as concentration of  $\text{Cu}^{2+}$  and density of glass, they are not large enough to change the qualitative nature of the result. Thus, the estimation of relative  $[\text{Cu}^{2+}]$  ratio in the glass by the peak extinction coefficient is not possible. The origin of these findings is discussed below. The areas of the integrated absorption bands

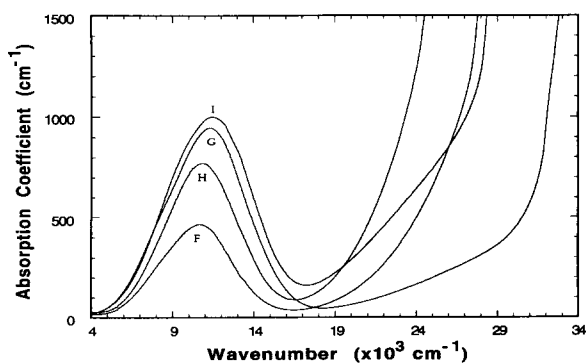


Fig. 2. Optical absorption spectra of oxidized and reduced glasses with 40% and 55% CuO batch composition. F–I, see Table 1.

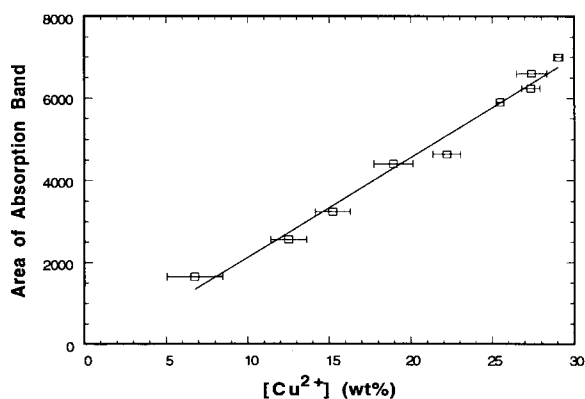


Fig. 3. Area of integrated absorption band as a function of  $\text{Cu}^{2+}$  concentration (wt%) in the glass.

were computed, and are shown plotted as a function of concentration of  $\text{Cu}^{2+}$  (wt%) in Fig. 3. The plot is linear, showing that the area is proportional to the concentration of  $\text{Cu}^{2+}$  in the glass. Thus, the area of integrated absorption band may be used to determine the relative content of  $\text{Cu}^{2+}$  in the glass.

## 4. Discussion

### 4.1. Ligand field of $\text{Cu}^{2+}$ coordination

It is well known that  $\text{Cu}^{2+}$  is present in glass and aqueous complexes in an octahedral coordination [24]. The five d-orbitals of copper, which have the same energy in the free gaseous ions, are split into two degenerate energy levels when coordinated octahedrally with six ligands, the orbitals being in the lower energy level ( ${}^2\text{T}_{2g}$ ) and in the higher energy state ( ${}^2\text{E}_g$ ) as shown in Fig. 4. In a regular octahedral complex without any distortion, the six ligands are equivalent, and a single absorption band corresponding to the electronic transition  ${}^2\text{E}_g \rightarrow {}^2\text{T}_{2g}$  should be observed. The energy difference between  ${}^2\text{E}_g$  and  ${}^2\text{T}_{2g}$  energy levels associated with this absorption band is usually denoted by  $10\text{Dq}$ . However, a lack of cubic symmetry results due to the Jahn–Teller effect, which states that for degenerate states the most symmetric configuration is unstable, and hence a tetragonal distortion is produced [24].

This effect results in an elongated tetragonal octahedral stereochemistry with four short in-plane bond lengths and two larger axial bond lengths. The lengths of two longer axial bonds along the  $z$ -axis grow with tetragonal distortion and as a limiting case one observes a square planar complex without  $z$ -axial bonds. In the tetragonal distortion of the octahedral coordination, the orbitals partly directed along the  $z$ -axis are preferentially occupied and more stable. Thus, the energy states of the latter orbitals are lowered, while those of other orbitals increase, since the complex is more tetragonally distorted. This produces additional splitting of the  $d$  orbital energy levels as shown in Fig. 4. As the degree of the tetragonal distortion increases, the splitting of the  $d$  orbital energy levels is enhanced, and thus the transition energies between energy levels change. However, the transition energy between the  $d_{xy}$  and  $d_{x^2-y^2}$  orbitals ( ${}^2B_{2g} \rightarrow {}^2B_{1g}$ ) remains constant regardless of the tetragonal distortion and is equal to  $10 Dq$  as in the case of an octahedral coordination without tetragonal distortion.

#### 4.2. Deconvolution of absorption band

As a result of the Jahn–Teller effect, more than one electronic transition is possible due to

the splitting of  $d$  orbital energy levels, as illustrated in Fig. 4. If multiple energy transitions contribute to the optical absorption spectra, then one expects a broad and asymmetrical absorption band (as observed in this study; see Figs. 1 and 2). Similar absorption bands have been found in  $Cu^{2+}$  complexes of other glasses and aqueous solutions [3–6,11,13–20,26]. This wide and asymmetric absorption band has been explained in terms of overlapping of two- or three-component absorption bands. Each component absorption band corresponds to a single electronic transition and depends upon the degree of tetragonal distortion.

This implies that the broad absorption band can be resolved into two- or three-component Gaussian absorption bands. In fact, the absorption bands of glasses containing copper as a dopant have been deconvoluted into two absorption bands, which for silicate glasses are centered at  $12\,600$  and  $8\,500\text{ cm}^{-1}$  [14], for borate glasses at  $12\,700$  and  $9\,000\text{ cm}^{-1}$  [4,14] and for nitrate glasses at  $12\,000$  and  $9\,000\text{ cm}^{-1}$  [6]. Three absorption bands at  $8\,500\text{ cm}^{-1}$ ,  $12\,000$  and  $13\,250\text{ cm}^{-1}$  were used to resolve the absorption band in cupric phosphate solutions, and these bands were assigned to the energy transitions  ${}^2B_{2g} \rightarrow {}^2B_{1g}$ ,  ${}^2A_{1g} \rightarrow {}^2B_{1g}$  and  ${}^2E_g \rightarrow {}^2B_{1g}$ , respectively [26]. However, these deconvolutions are not applicable to

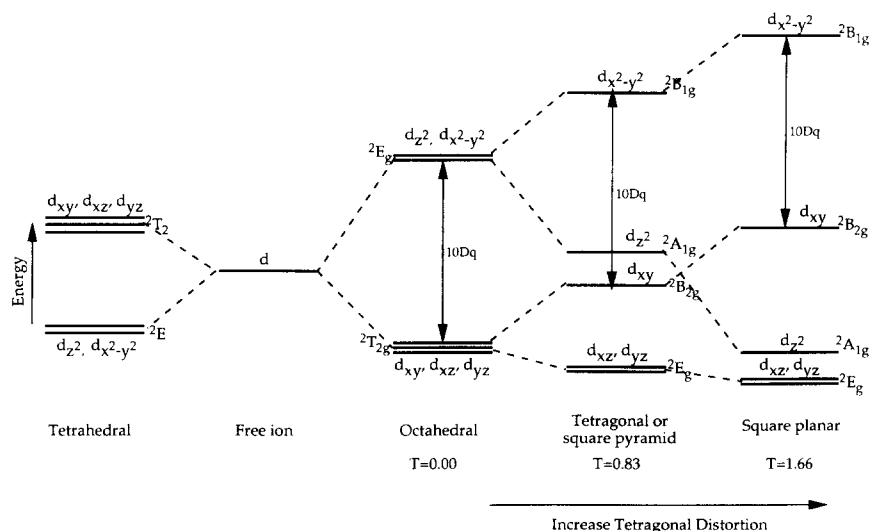


Fig. 4. Energy level diagram of  $Cu^{2+}$  in different ligand fields.

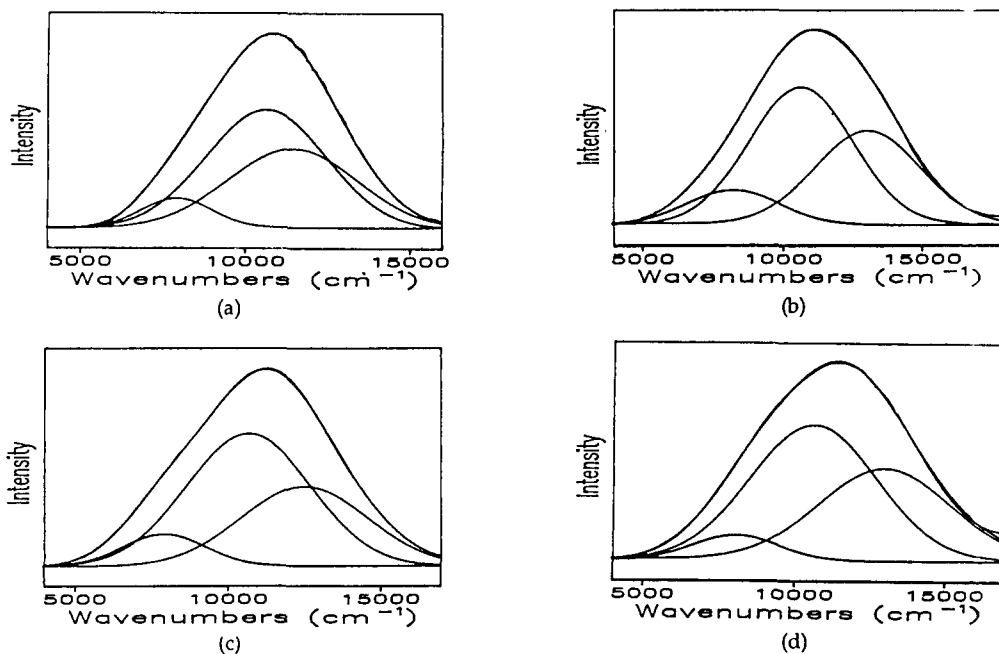


Fig. 5. Examples of deconvolution of absorption band of (a) A, (b) E, (c) G and (d) I glasses.

the absorption band observed in the present study since the position and width of this absorption band differs from those seen earlier. Thus, other deconvolutions into two- or three-component Gaussian curves have been attempted using curve-fitting software. This software was developed at the University of Arizona [27] and provides for user-defined asymmetric Gaussian curve fits of up to nine overlapped spectral bands at one time. It has the option of choosing any of the

independent variables such as peak wavenumber, left and right full width at half-maximum (FWHM), and intensity for each band in order to achieve the best fit. Curve fittings were tried to fit the absorption band using two or three absorption bands. Better resolution and more reliable results were obtained by use of three-component absorption bands at near 8000, 10600 and 12000  $\text{cm}^{-1}$  rather than two-component absorption bands. Examples of the deconvolutions of the

Table 3  
Deconvoluted absorption bands and degree of tetragonal distortion

Glass	First band ( $\text{cm}^{-1}$ )	Second band ( $\text{cm}^{-1}$ )	Third band ( $\text{cm}^{-1}$ )	$T = \frac{\text{third band}}{\text{second band}}$
A	11 640	10 640	7920	0.74
B	12 140	10 640	8000	0.75
C	12 520	10 660	8080	0.76
D	12 720	10 640	8120	0.76
E	13 080	10 680	8240	0.77
F	11 920	10 640	7800	0.73
G	12 560	10 680	7920	0.74
H	12 320	10 680	8080	0.76
I	12 960	10 640	8320	0.78
Energy transition	${}^2E_g \rightarrow {}^2B_{1g}$	${}^2B_{2g} \rightarrow {}^2B_{1g}$	${}^2A_{1g} \rightarrow {}^2B_{1g}$	

absorption bands are illustrated in Fig. 5 and the results are presented in Table 3. All deconvoluted bands have similar characteristics, with a strong band centered at approximately  $10\,600\text{ cm}^{-1}$  and weak ones at lower and higher wavenumbers. As the  $[\text{Cu}^{2+}]$  ratio in the glass for each composition is increased, the low and high wavenumber bands shift to higher wavenumber, but the position of the central band remains unchanged. From the inspection of energy level diagram shown in Fig. 4, one notes that the energy absorbed in the energy transition  ${}^2\text{B}_{2g} \rightarrow {}^2\text{B}_{1g}$ ,  $10\text{ Dq}$ , is constant irrespective of the degree of the tetragonal distortion and is dependent on the types of ligand and metal ion [24,25]. Thus, the strong absorption band at  $10\,600\text{ cm}^{-1}$  seems to correspond to the energy transition  ${}^2\text{B}_{2g} \rightarrow {}^2\text{B}_{1g}$ , and hence the bands at  $8000$  and  $12\,000\text{ cm}^{-1}$  are assigned to  ${}^2\text{A}_{1g} \rightarrow {}^2\text{B}_{1g}$  and  ${}^2\text{E}_g \rightarrow {}^2\text{B}_{1g}$ , respectively. This assignment is different from those made in cupric phosphate solution [26].

From the above results, it is clear why the extinction coefficient at the absorption band peak is not simply related to the  $[\text{Cu}^{2+}]$  ratio in the glass and glass composition. Since the absorption band consists of three-component absorption bands, whose peak positions, intensities and widths depend upon the extent of tetragonal distortion of  $\text{Cu}^{2+}$  coordination, neither the peak wavenumber nor the peak extinction coefficient of the absorption band will be related simply to the concentration of  $\text{Cu}^{2+}$  in the glass. However, the area of the integrated absorption band must increase with enhancing the concentration of  $\text{Cu}^{2+}$  in the glass as shown in Fig. 3.

#### 4.3. Variations of absorption band

The peak position of the absorption band which is determined by the coordination of  $\text{Cu}^{2+}$  and its environment, is about  $11\,000\text{ cm}^{-1}$  and varies with the  $[\text{Cu}^{2+}]$  ratio and glass composition, as shown in Table 2. The peak wavenumber grows with increasing  $[\text{Cu}^{2+}]$  ratio and CuO content in the glass, but it does not change significantly. These observations also hold for the deconvoluted bands. The absorption band broadens with

increasing  $[\text{Cu}^{2+}]$  ratio in the glass. As the  $[\text{Cu}^{2+}]$  ratio and CuO content in the glass are increased, the positions of the low and high wavenumber (third and first) deconvoluted bands shift to higher wavenumber and, thus, the peak wavenumber of the absorption band increases. The shift of the first deconvoluted band to higher wavenumber as well as the broadening of the second deconvoluted band enhance the width of the absorption band as the  $[\text{Cu}^{2+}]$  ratio in the glass is increased for each composition.

The shape and peak position of the absorption band of copper-doped glasses have been found to be sensitive to glass composition [3–20]. For phosphate glasses and phosphate solutions containing a small quantity of copper, the peak position of the absorption band has been found to be generally located about  $12\,000\text{ cm}^{-1}$  [15–19,26]. This peak wavenumber of the absorption band is somewhat larger than those of the copper phosphate glasses studied here. This may be due to overlapping of different component absorption bands as shown in cupric phosphate solution [26]. However, the shape and width of the absorption band are very similar for both copper-doped glasses and copper phosphate glasses, which contain a large copper content.

#### 4.4. Tetragonal distortion of $\text{Cu}^{2+}$

From the energy level diagram shown in Fig. 4, one observes that the  ${}^2\text{A}_{1g} \rightarrow {}^2\text{B}_{1g}$  energy transition is most sensitive to the change in the degree of tetragonal distortion. Thus, the ratio of the peak wavenumber of the third band corresponding to this energy transition to the peak wavenumber of the second band (which is constant  $10\text{ Dq}$ ),  $T$ , can be used to measure the extent of the tetragonal distortion. A similar ratio was used to determine the degree of tetragonal distortion in a cupric phosphate solution. [26] As the complex is more distorted,  $T$  increases from zero for regular octahedral complex to 1.66 for square planar complex [25]. These ratios have been computed for the copper phosphate glasses and they range from 0.74 to 0.78 as listed in Table 3. Thus, the coordination of  $\text{Cu}^{2+}$  in copper phosphate glass is a distorted octahedral co-

ordination whose tetragonal distortion is less than that of the square pyramid. This coordination is the same as observed in crystalline copper phosphates [28]. The  $T$  values are slightly dependent upon the  $[\text{Cu}^{2+}]$  ratio in the glass and glass composition, but much less than in phosphate solutions [26]. In general, the tetragonal distortion increases, but not significantly, with increasing  $[\text{Cu}^{2+}]$  ratio and CuO content in the glass.

#### 4.5. Color of glasses

The color of the prepared glasses ranges from brown to green to blue as the  $[\text{Cu}^{2+}]$  ratio of the glass is increased for each glass composition. The color of glasses containing copper is known to be determined by the absorption band in the visible and near-infrared spectral range. However, the color change in the glass depending on the  $[\text{Cu}^{2+}]$  ratio in the glass has not been investigated. Since the peak position of the absorption band does not vary significantly with the  $[\text{Cu}^{2+}]$  ratio in the glass, it is not responsible for the color changes in the glass. On the other hand, the tail of the UV absorption edge extends into the visible spectrum region (400–700 nm) and effects the color changes in the glass. In addition to the visible absorption band originating from  $\text{Cu}^{2+}$ , the tail of the UV absorption band produced by crystal field of  $\text{Cu}^{1+}$  in the glass [21,23] extends into the visible spectrum region and thus contributes to the color of the glass. For the oxidized glass, the absorption band of  $\text{Cu}^{1+}$  is negligible in the visible spectrum and a green or blue color is observed. As the  $[\text{Cu}^{2+}]$  ratio in the glass decreases, the effect of the absorption band of  $\text{Cu}^{1+}$  is enhanced and the color of glass changes to brown or tan. Since the extension of the absorption band of  $\text{Cu}^{1+}$  into the visible region overlaps the absorption band of  $\text{Cu}^{2+}$ , one observes a minimum absorption between the visible absorption band and UV absorption edge. The wavenumbers of minimum absorption are listed in Table 2, and one observes that they fall in the visible region for all glasses prepared. Fig. 6 shows the variation of the minimum absorption position as a function of the  $[\text{Cu}^{2+}]$  ratio in the glass. The position of minimum absorption shifts to larger wavenumbers as

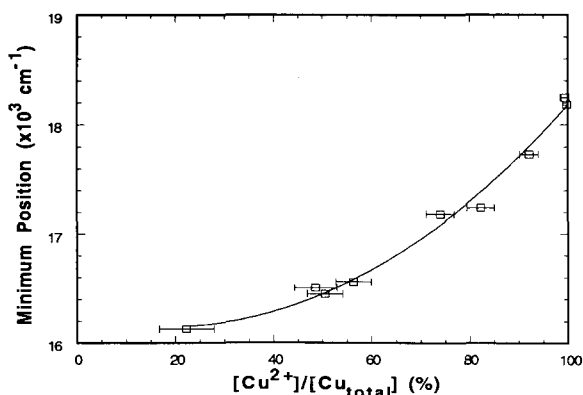


Fig. 6. Position of minimum absorption as a function of  $[\text{Cu}^{2+}]$  ratio in the glass.

the  $[\text{Cu}^{2+}]$  ratio in the glass increases, regardless of the glass composition. This variation agrees well with the change in the color of the glass. The shift in the position of minimum absorption with glass composition has been given for other copper phosphate glasses in terms of the influence of glass composition upon the  $[\text{Cu}^{2+}]$  ratio in the glass [20]. The present results support this description of the behavior of the change in the wavenumber of minimum absorption as a function of glass composition.

#### 5. Summary and conclusions

Copper phosphate glasses show color due to an absorption band in the visible through near-infrared region of the optical absorption spectra. The absorption band exhibits similar characteristics but smaller peak wavenumber compared with those of copper-doped phosphate glasses and solutions. The absorption band consists of three-component Gaussian bands, each of which corresponds to an energy transition between assigned energy levels in a tetragonally distorted octahedral complex, and is responsible for the relatively large width and asymmetry of the absorption band. It is found that the tetragonal distortion of the octahedral coordination of  $\text{Cu}^{2+}$  in the copper phosphate glass increases slightly as the  $[\text{Cu}^{2+}]$  ratio and CuO content in the glass increase. The position of minimum absorption pro-



duced by the overlapping of the absorption bands of  $\text{Cu}^{1+}$  and  $\text{Cu}^{2+}$  increases with the  $[\text{Cu}^{2+}]$  ratio and is responsible for the color changes in the glass.

The authors would like to thank the Advanced Technology Center of Donnelly Corporation in Tucson, AZ, USA, for permitting the use of their Optical Absorption Spectrophotometer. They also would like to thank Professor J.E. Pemberton, Department of Chemistry, University of Arizona, for permitting the use of the curve-fitting software.

## 6. References

- [1] W.A. Weyl, *Coloured Glasses* (Society of Glass Technology, Sheffield, UK, 1951).
- [2] T. Bates, in: *Modern Aspects of the Vitreous State*, Vol. 2, ed. J.D. Mackenzie (Butterworth, Washington, DC, 1962) p. 250.
- [3] C.R. Bamford, *Phys. Chem Glasses* 3 (1962) 189.
- [4] R. Juza, H. Seidel and J. Tiedemann, *Angew. Chem. Int. Edit.* 5 (1966) 85.
- [5] A. Paul, *Phys. Chem. Glasses* 11 (1970) 159.
- [6] R.F. Bartholomew and R.E. Tischer, *J. Am. Ceram. Soc.* 53 (1970) 130.
- [7] P.C. Schultz, *J. Am. Ceram. Soc.* 57 (1974) 309.
- [8] J.A. Duffy, *J. Am. Ceram. Soc.* 60 (1977) 440.
- [9] S. Sakka, K. Kamiya and H. Yoshikawa, *J. Non-Cryst Solids* 27 (1978) 289.
- [10] H. Hosono, H. Kawazoe and T. Kanazawa, *J. Non-Cryst. Solids* 33 (1979) 103.
- [11] A.K. Bandyopadhyay, *J. Mater. Sci.* 16 (1981) 189.
- [12] D. Shen, K. Wang, X. Huang, Y. Chen and J. Bai, *J. Non-Cryst Solids* 52 (1982) 151.
- [13] A.A. Ahmed, A.F. Abbas and F.A. Moustafa, *Phys. Chem. Glasses* 24 (1983) 43.
- [14] A. Duran and J.M. Fernandez Navarro, *Phys. Chem Glasses* 26 (1985) 126.
- [15] J.C. Haddon, E.A. Rogers and D.J. Williams, *J. Am. Ceram. Soc.* 52 (1969) 52.
- [16] T. Maekawa, T. Yokokawa and K. Niwa, *Bull. Chem. Soc. Jpn.* 42 (1969) 2102.
- [17] M. Berretz and S.L. Holt, *J. Am. Ceram. Soc.* 61 (1978) 136.
- [18] A. Klonkowski, *Phys. Chem. Glasses* 22 (1981) 163.
- [19] A. Klonkowski, *Phys. Chem. Glasses* 26 (1981) 11.
- [20] E.E. Kjawaja, M.N. Khan, A.A. Kutub and C.A. Hogarth, *Int. J. Electron.* 58 (1985) 471.
- [21] R. Debnath, J. Chaudhury and S.C. Bera, *Phys. Status Solidi (B)* 157 (1990) 723.
- [22] B.S. Bae and M.C. Weinberg, *J. Appl. Phys.* 73 (1993) 7760.
- [23] B.S. Bae and M.C. Weinberg, *J. Am. Ceram. Soc.* 74 (1991) 3039.
- [24] F.A. Cotton and G. Wilkinson, *Advanced Inorganic Chemistry*, 5th Ed. (Wiley-Interscience, New York, 1988).
- [25] F. Baselo and R.G. Pearson, *Mechanisms of Inorganic Reactions*, 2nd Ed. (Wiley, New York, 1967) p. 65.
- [26] J.E. Spessard, *Spectrochim. Acta* 25A (1969) 731.
- [27] LESSASOFT, University of Arizona (1986).
- [28] B.J. Hathaway and P.G. Hodgson, *J. Inorg. Nucl. Chem.* 35 (1973) 4071.